Journal of Sound and Vibration (1999) **225**(2), 391–398
Article No. jsvi.1998.1851, available online at http://www.idealibrary.com.on IDEAL ®

LETTER TO THE EDITOR

VIBRATION CONTROL OF A CANTILEVERED BEAM VIA HYBRIDIZATION OF ELECTRO-RHEOLOGICAL FLUIDS AND PIEZOELECTRIC FILMS

YONG-KUN PARK

Department of Mechanical Design, *Myongji College*, *Seoul* 120-728, *Korea*

AND

SEUNG-BOK CHOI

Smart Structures and Systems Laboratory,
Department of Mechanical Engineering, *Inha University*, *Incheon* 402-751, *Korea*

(*Received* 28 *August* 1996, *and in final form* 29 *June* 1998)

1. INTRODUCTION

Recently, an increasingly insatiable demand in the international marketplaces for higher-performance in structural and mechanical systems at various fields such as aerospace, defense, automotive and manufacturing industries has evolved ultra-advanced structures, so called smart structures [1]. The smart structures have their inherent adaptive capabilities, which are of multi-disciplinary areas pertaining to design, fabrication, sensing, actuating, and microprocessor-based real-time control. As one of principal ingredients of the smart structures, the actuating technology is typically exploited to dramatically tune global mechanical properties of the structures, or else to dynamically tailor the shapes of the structures in an orchestrated manner. As of now, electro-rheological fluids, piezoelectric materials (film or ceramic), and shape memory alloys have been widely investigated as prominent actuator candidates in vibration control of structural systems.

On the other hand, each actuator has diverse characteristics, with distinct advantages and disadvantages. In order to achieve diverse and stringent performances under constraints of weight, size, shape, and energy consumption, various functional technologies with a hybrid design philosophy are required. Thereby, by performing a judicious selection, smart structure designers can synthesize numerous classes of hybrid actuation systems to satisfy a broad range of specifications, which cannot be accomplished by developing a single class of actuator system alone. This study exhibits a proof-of-concept investigation on vibration control of a cantilevered beam consisting of an electro-rheological fluid actuator (ERFA) and a piezoelectric film actuator (PFA). Firstly, a hybrid smart structure (HSS) is fabricated by inserting a starch/silicone oil-based electro-rheological (ER) fluid into a hollow composite beam and perfectly bonding two piezoelectric films on the outer surfaces of the structure as an actuator and a sensor. Then, control schemes for the ERFA and the PFA are synthesized on the basis of field-dependent frequency responses and neural networks respectively.

0022–460X/99/320391 + 08 $30.00/0

Subsequently, vibration performances in view of the suppression of tip deflections are evaluated in order to demonstrate the control effectiveness of the proposed hybrid actuation methodology.

2. FORMULATION OF CONTROL SCHEME

2.1. *ERFA* (*electro-rheological fluid actuator*)

Embedded in voids of host materials, the ERFA enables stiffness and damping characteristics of the ER fluid-based structures to be instantly changed by imposing electric fields on the fluid domain. Thus, the field-dependent frequency responses of the structures can be obtained from either modelling or experiment. On the basis of the field-dependent responses a control scheme is fabricated which provides actively minimized responses over broad frequency ranges by avoiding resonance situations under variable excitations [2].

Figure 1 shows the inferred frequency responses at the tip position by applying the electric fields. In fact, frequency response means a relative deflection over frequency span under the forced vibration. So, Figure 1 exhibits how to determine the input field for actively minimizing tip deflections of the HSS. By a selection of the minimizing envelopes (○○○○○) among the three field-dependent responses at each excitation frequency, both the frequency bandwidth and the desired electric fields corresponding to the minimizing envelopes are obtained. This algorithm can be expressed as the following logical statement.

$$\text{IF} \quad \tilde{\omega}_i \leqslant \tilde{\omega} < \tilde{\omega}_{i+1}, \quad \text{THEN} \quad E_d = E_i \tag{1}$$

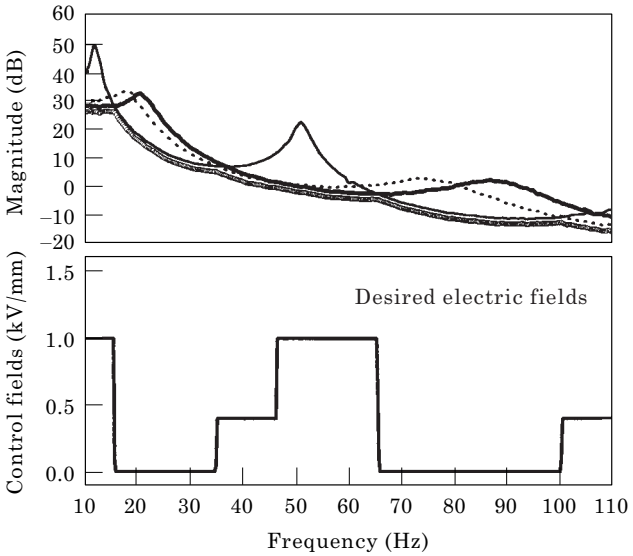

Figure 1. Control strategy for the ERFA. ——, 0·0 kV/mm; -----, 0·4 kV/mm; ——, 1·0 kV/mm; ○○○○○, desired response.

where $\tilde{\omega}$ denotes the excitation frequency and E_i represents the applied electric field to the desirable electric field of E_d. Thus, the control electric field of the ERFA for the proposed HSS under the given electric fields is determined by

$$\begin{aligned}
&\text{IF} \quad 0{\cdot}0\ \text{Hz} \leqslant \tilde{\omega} < 16{\cdot}1\ \text{Hz}, \quad \text{THEN} \quad E_d = 1{\cdot}0\ \text{kV/mm}\\
&\text{IF} \quad 16{\cdot}1\ \text{Hz} \leqslant \tilde{\omega} < 34{\cdot}5\ \text{Hz}, \quad \text{THEN} \quad E_d = 0{\cdot}0\ \text{kV/mm}\\
&\text{IF} \quad 34{\cdot}5\ \text{Hz} \leqslant \tilde{\omega} < 45{\cdot}3\ \text{Hz}, \quad \text{THEN} \quad E_d = 0{\cdot}4\ \text{kV/mm}\\
&\text{IF} \quad 45{\cdot}3\ \text{Hz} \leqslant \tilde{\omega} < 65{\cdot}5\ \text{Hz}, \quad \text{THEN} \quad E_d = 1{\cdot}0\ \text{kV/mm}\\
&\text{IF} \quad 65{\cdot}5\ \text{Hz} \leqslant \tilde{\omega} < 99{\cdot}6\ \text{Hz}, \quad \text{THEN} \quad E_d = 0{\cdot}0\ \text{kV/mm}\\
&\text{IF} \quad 99{\cdot}6\ \text{Hz} \leqslant \tilde{\omega} < 110{\cdot}0\ \text{Hz}, \quad \text{THEN} \quad E_d = 0{\cdot}4\ \text{kV/mm}
\end{aligned} \tag{2}$$

By activating this algorithm of avoiding resonance phenomenon, a minimized deflection over the focused frequency range can be obtained. This control scheme also indicates that the effectiveness relies on the field-dependent elastodynamic properties and external excitations as well.

2.2. *PFA* (*piezoelectric film actuator*)

On the other hand, the PFA produces a negative voltage to generate positive strains in piezoelectric actuators resulting in a moment counteracting the positive deflection of the structure and vice versa [3, 4]. As for the PFA, a neuro-sliding mode controller to determine a control voltage is adopted, which possesses the feasibility of an experimental implementation with only system output.

Figure 2 indicates a neuro-sliding mode controller (NSC) consisting of a three-layer neural network, with 2 neurons in the input layer (i), 5 neurons in the hidden layer (j), and 1 neuron in the output layer (k). As is well known, the neural

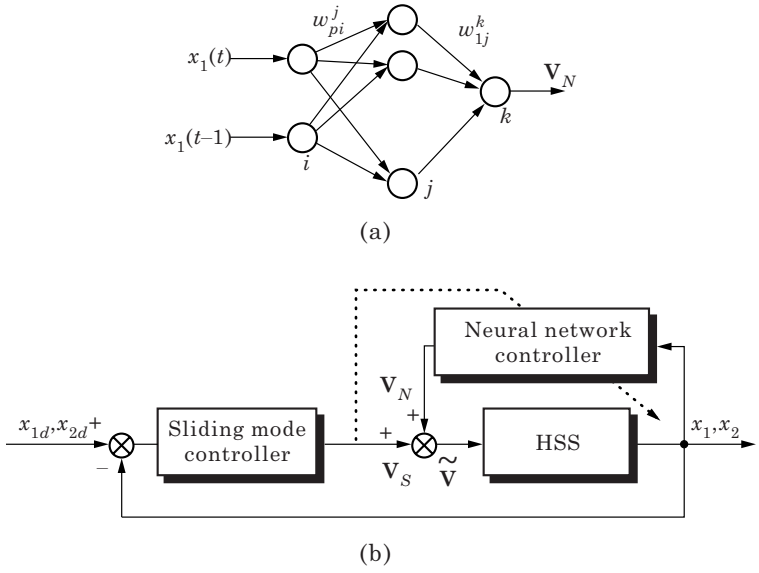

Figure 2. Neuro-sliding mode controller for the PFA. (a) Architecture; (b) block diagram.

network learning is largely employed in off-line state for parameter identification under a given desired value. In this study, the goal of neural network learning is to determine not a desired response but a desired control voltage $\tilde{V}$ for the PFA. As a matter of fact, a desired controller is not known in advance especially when a system includes disturbances and uncertainties. So, a real-time learning mechanism based on the idea of sliding mode and Lyapunov stability is employed to create a desired controller [5, 6]. So, δ_1^k to learn a neural network is defined as

$$\delta_1^k = S_1 + \dot{S}_1. \tag{3}$$

Herein, under consideration of vibration performance, maximum input voltage, and excitation magnitude, a sliding surface is chosen as $S_1 = 10e_1 + e_2$ where $e_1 = x_1 - x_{1d}$ and $e_2 = x_2 - x_{2d}$. The state variables x_1 and x_2 represent actual tip deflection and velocity, respectively. In order to suppress tip deflection under the forced vibration, the desired deflection x_{1d} and velocity x_{2d} are chosen as zero.

From the learning algorithm of error back propagation, the incremental changes, i.e., Δw_{pi}^j and Δw_{1j}^k of the weights for the hidden and output layers, respectively, are obtained as follows:

(i) between the input and hidden layers

$$\Delta w_{pi}^j = \eta \delta_1^k w_{1j}^k O_p^j (1 - O_p^j) X_i, \qquad O_p^j = f_j(net_p^j), \qquad net_p^j = \sum_{i=1}^{2} w_{pi}^j X_i,$$

$$(p = 1, 2, \ldots, 5) \tag{4}$$

(ii) between the hidden and output layers

$$\Delta w_{1j}^k = \eta \delta_1^k O_p^j, \qquad O_1^k = f_k(net_1^k), \qquad net_1^k = \sum_{p=1}^{5} w_{1p}^k O_p^j. \tag{5}$$

In the above, X_i denotes inputs for the hidden layers chosen as deflection $x_1(t)$, and previous deflection $x_1(t-1)$. The learning rate η, related to convergence speed of the learning algorithm, is chosen as 0·5. In this model, the neuron of the output layer k has a linear mapping activation function, $f_k(z) = 5 \cdot z$, while the neurons of the hidden layers j have a sigmoid mapping activation function $f_j(z) = 2/[1 + \exp(-5 \cdot z)] - 1$. net_p^j and net_1^k are inputs corresponding to the mapping functions. O_p^j and O_1^k are outputs of the hidden and output layers respectively. Now, as evident from the block diagram, the control voltage $\tilde{V}$ for the PFA is determined by

$$\tilde{V} = V_N + V_S = O_1^k + K_1 S_1. \tag{6}$$

In this study, the control voltage is limited to 1·5 kV on account of an allowable maximum voltage to the PFA. The control gain K_1 associated with the sliding hyperplane S_1 is appropriately chosen as 80 under consideration of vibration performance, maximum input voltage, and excitation magnitude.

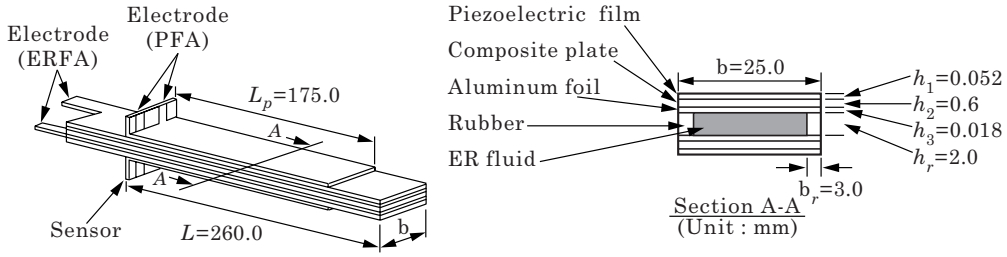

Figure 3. Schematic diagram of the proposed HSS.

3. EXPERIMENTAL PROCEDURES AND RESULTS

Figure 3 illustrates a schematic diagram of the proposed HSS. The specimen consists of two glass/epoxy composite plates, rubber, aluminum foils, acrylic, an ER fluid (starch and silicone oil-based), and two piezoelectric films. The dimension variables are defined as follows; L and L_p are the length of the specimen and the piezoelectric film respectively. b and b_r denote the width of the specimen and the silicone rubber respectively. h_1, h_2, h_3, and h_r represent the thickness of the piezoelectric film, the composite plates, the aluminum foil, and the rubber respectively. The composite plates act as the host material to hold the rigidity of the specimen. The two piezoelectric films bonded on the upper and lower surfaces of the specimen are employed as the PFA and the sensor. The inner surfaces of the specimen are coated with the aluminum foil to furnish electrodes for the ERFA. The control voltages for the PFA and the fields for the ERFA may possibly interfere with each other. Thus, the composite plates also have to be activated as a dielectric. The rubber as a seal to hold the integrity of the

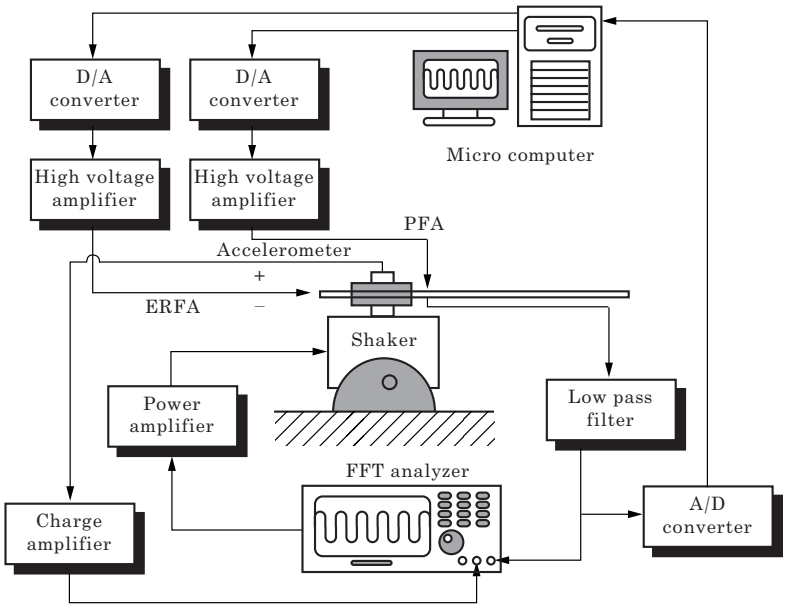

Figure 4. Experimental set-up.

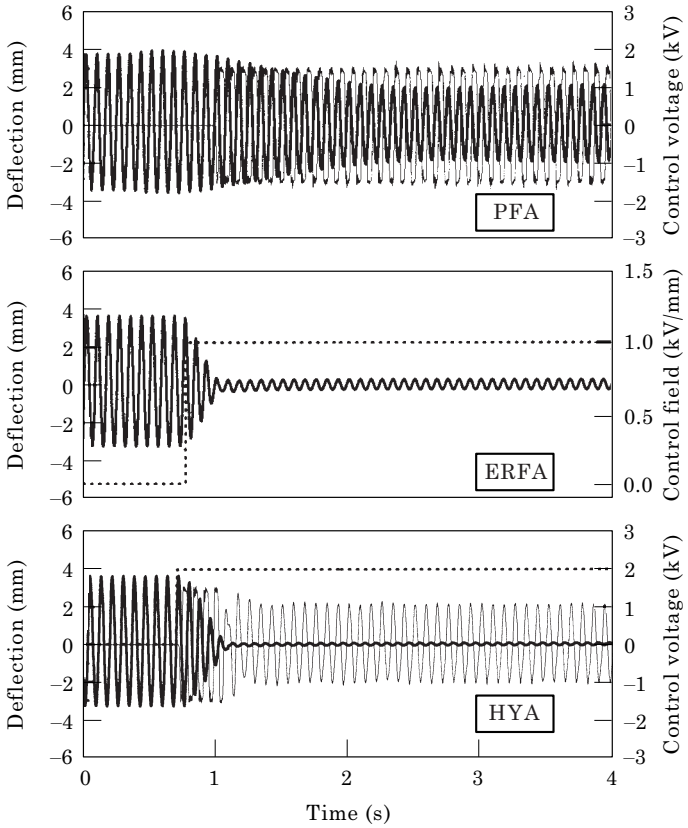

Figure 5. Forced vibration responses at the first mode in the time domain.

specimen is also used to adjust the volume fraction of the ER fluid relative to the total volume of the structure.

Figure 4 demonstrates the experimental apparatus and associated instrumentation to investigate vibration performances for the HSS. The cantilevered specimen is clamped in the fixture bolted down on the top of the shaker (MB PM-50). Two signals from both the accelerometer (Dytran 3152C) and the lower piezoelectric film (sensor) are used to obtain transfer functions at random excitation of RMS of 1·10 m/s^2. On the other hand, the signal from the sensor is also fed back to the microcomputer through the A/D converter (Keithely, DAS 20) to provide the information on excitation disturbances and tip deflections. With the aid of the feedback signal, both the fields for the ERFA and the control voltages for the PFA are determined in the microcomputer with the proposed active control strategies. Two desired control inputs for suppressing the tip deflection are independently supplied to the specimen via the D/A converters and two high voltage amplifiers (Trek 609A-3) with a magnification of 1000.

Figure 5 presents the forced vibration responses in the time domain under excitation of the fundamental natural frequency of 12·0 Hz. The tip deflection of 3·90 mm at the open loop is reduced to 2·10, 0·37 and 0·17 mm by activating the PFA, the ERFA, and the hybridization of two actuators (HYA) respectively. In

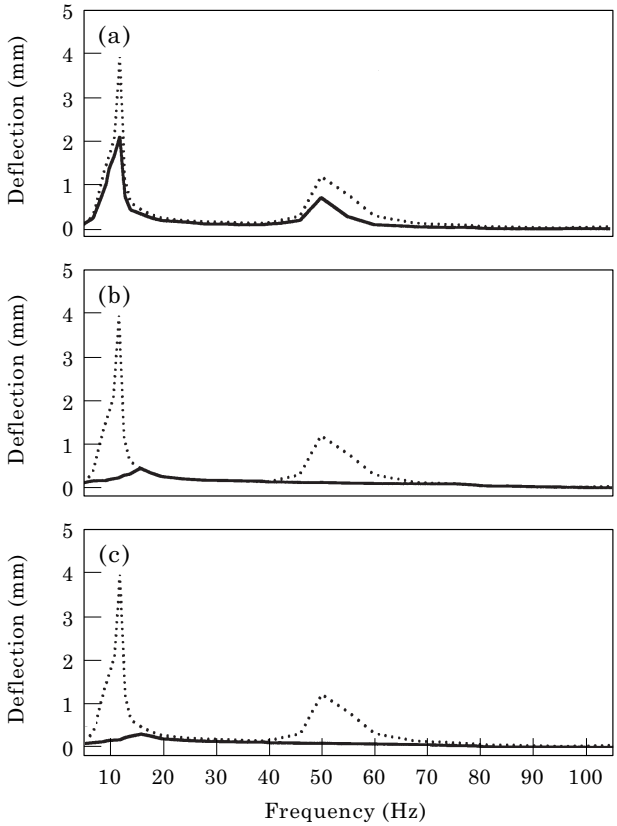

Figure 6. Forced vibration responses in the frequency domain. -----, Open loop; ——, (a) PFA; (b) ERFA; (c) HYA.

addition, Figure 6 provides the forced vibration responses in the frequency domain over the focused frequency ranges by applying the PFA, the ERFA, and the HYA. As easily expected, due to resonance avoidance the control effect of the ERFA in the neighborhood of natural frequencies is greater than that of the PFA. However, because the ERFA changes only elastodynamic properties of the structure with no actual physical force, a non-zero deflection always exists. With the addition of the PFA, the drawback of a semi-active actuation of the ERFA can be overcome.

4. CONCLUSIONS

A proof-of-concept investigation on the active vibration control of the hybrid smart structures was undertaken through the formulation of control schemes and experimental implementation. Vibration control performances in view of suppression of tip deflections under the forced vibration were evaluated. With the hybridization of two actuators with the ERFA and the PFA, superior results were accomplished in the sense of tailoring elastodynamic response characteristics of the smart structure rather than a single class of actuation system alone. This class of the hybrid actuator system can provide the possibility that any combination of existing smart materials may furnish a certain hybrid smart structure satisfying

required system performances under constraints and severe environmental conditions.

REFERENCES

1. M. V. Gandhi and B. S. Thompson 1992 *Smart Materials and Structures*. London: Chapman & Hall.
2. S. B. Choi and Y. K. Park 1994 *Journal of Sound and Vibration* **172**, 428. Active vibration control of a cantilevered beam containing an electro-rheological fluid.
2. T. Bailley and J. E. Hubbard, Jr. 1985 *AIAA Journal of Guidance Control, and Dynamics* **8**(5), 605. Distributed piezoelectric-polymer active vibration control of a cantilever beam.
4. S. B. Choi 1995 *AIAA Journal* **33**(3), 564. Alleviation of chattering in flexible beam control via piezofilm actuator and sensor.
5. Y. S. Tarng, S. T. Hawang and Y. S. Wang 1994 *Int. J. Mach. Tools Manufact.* **34**(4), 453. A neural network controllers for constant turning force.
6. K. P. Venugopal and S. M. Smith 1993 *ACC*. San Francisco, CA, 84. A feed-back scheme for improving dynamic response of neuro-controllers.